The *sys-1* and *sys-3* Genes Cooperate With Wnt Signaling to Establish the Proximal-Distal Axis of the *Caenorhabditis elegans* Gonad

Kellee R. Siegfried,*,[1] Ambrose R. Kidd III,† Michael A. Chesney‡ and Judith Kimble*,†,‡,§,[2]

**Laboratory of Genetics,* †*Program in Cellular and Molecular Biology,* ‡*Department of Biochemistry and* §*Howard Hughes Medical Institute, University of Wisconsin, Madison, Wisconsin 53706-1544*

Manuscript received July 22, 2003
Accepted for publication October 10, 2003

ABSTRACT

To form the proximal-distal axis of the *C. elegans* gonad, two somatic gonadal precursor cells, Z1 and Z4, divide asymmetrically to generate one daughter with a proximal fate and one with a distal fate. Genes governing this process include the *lin-17 frizzled* receptor, *wrm-1*/β-catenin, the *pop-1*/TCF transcription factor, *lit-1/nemo-like kinase*, and the *sys-1* gene. Normally, all of these regulators promote the distal fate. Here we show that nuclear levels of a *pop-1* GFP fusion protein are less abundant in the distal than in the proximal Z1/Z4 daughters. This POP-1 asymmetry is lost in mutants disrupting Wnt/MAPK regulation, but retained in *sys-1* mutants. We find that *sys-1* is haplo-insufficient for gonadogenesis defects and that *sys-1* and *pop-1* mutants display a strong genetic interaction in double heterozygotes. Therefore, *sys-1* is a dose-sensitive locus and may function together with *pop-1* to control Z1/Z4 asymmetry. To identify other regulatory genes in this process, we screened for mutants resembling *sys-1*. Four such genes were identified (*gon-14*, *-15*, *-16*, and *sys-3)* and shown to interact genetically with *sys-1*. However, only *sys-3* promotes the distal fate at the expense of the proximal fate. We suggest that *sys-3* is a new key gene in this pathway and that *gon-14*, *gon-15*, and *gon-16* may cooperate with POP-1 and SYS-1 at multiple stages of gonad development.

ORGANOGENESIS requires the careful orchestration of cell divisions, cell positions, and cell fates. An early step in organogenesis is the establishment of organ axes. Most organs are oriented with respect to the primary body axes (*e.g.*, anterior-posterior, dorsal-ventral, and left-right), at least during early organ development. However, some organs acquire an organ-specific axis that does not correspond to primary body axes. For example, limbs or appendages acquire a proximal-distal (PD) axis (*e.g.*, Niswander 2002), as does the *Caenorhabditis elegans* gonad (*e.g.*, Hubbard and Greenstein 2000). The mechanisms for establishing organ axes that depart from primary body axes are poorly understood.

We have focused on *C. elegans* gonadogenesis to investigate controls governing early organogenesis and formation of a novel, organ-specific axis. The cellular events that establish the initial gonadal axes were revealed by early lineage studies (Kimble and Hirsh 1979). Briefly, the gonad develops from a four-celled gonadal primordium, consisting of two somatic gonadal precursor cells called Z1 and Z4 and two primordial germ cells (PGCs; Figure 1A; Hubbard and Greenstein 2000). Z1 occupies the anterior right pole and Z4 occupies the posterior left pole of the primordium; moreover, Z1 and Z4 extend processes ventrally to meet beneath the PGCs (Figure 1, A and B). Therefore, the gonadal primordium has anterior-posterior, dorsal-ventral, and left-right axes. Z1 and Z4 undergo coordinated and virtually invariant cell divisions, cell fate decisions, and patterning to generate the adult somatic gonad. In hermaphrodites, the mature gonad is a symmetrical structure, with two ovotestes, or "arms," emanating from central somatic tissues (*i.e.*, uterus and spermatheca), whereas in males, the gonad is asymmetric, with a single testis extending from posterior somatic tissues (*i.e.*, seminal vesicle, vas deferens). Nonetheless, the gonads of both sexes have related PD axes: the germ line is distal and somatic gonadal tissues are proximal (Figure 1, D and F). However, the hermaphrodite gonad possesses two opposing PD axes, while the male has a single PD axis (Figure 1, D and F, arrows).

The first step in establishing the gonadal PD axes is the asymmetric cell division of Z1 and Z4 (Figure 1). In each sex, Z1 and Z4 generate one daughter with a distal fate and one with a proximal fate (Figure 1B). In both hermaphrodites and males, the distal daughter generates a distal tip cell (DTC) and the proximal daughter generates either a cell with anchor cell (AC) potential in hermaphrodites or a cell with linker cell (LC) potential in males (Figure 1, B, D, and F). The DTCs signal germline proliferation in both sexes (Kimble and White 1981). In hermaphrodites, the two DTCs also lead elongation to generate two gonadal arms, whereas in males, the single LC leads elongation to

[1]*Present address:* Max-Planck-Institut für Entwicklungsbiologie, Abt. Genetik, Spemannstrasse 35, 72076 Tübingen, Germany.

[2]*Corresponding author:* Department of Biochemistry, 433 Babcock Dr., University of Wisconsin, Madison, WI 53706-1544.
E-mail: jekimble@facstaff.wisc.edu

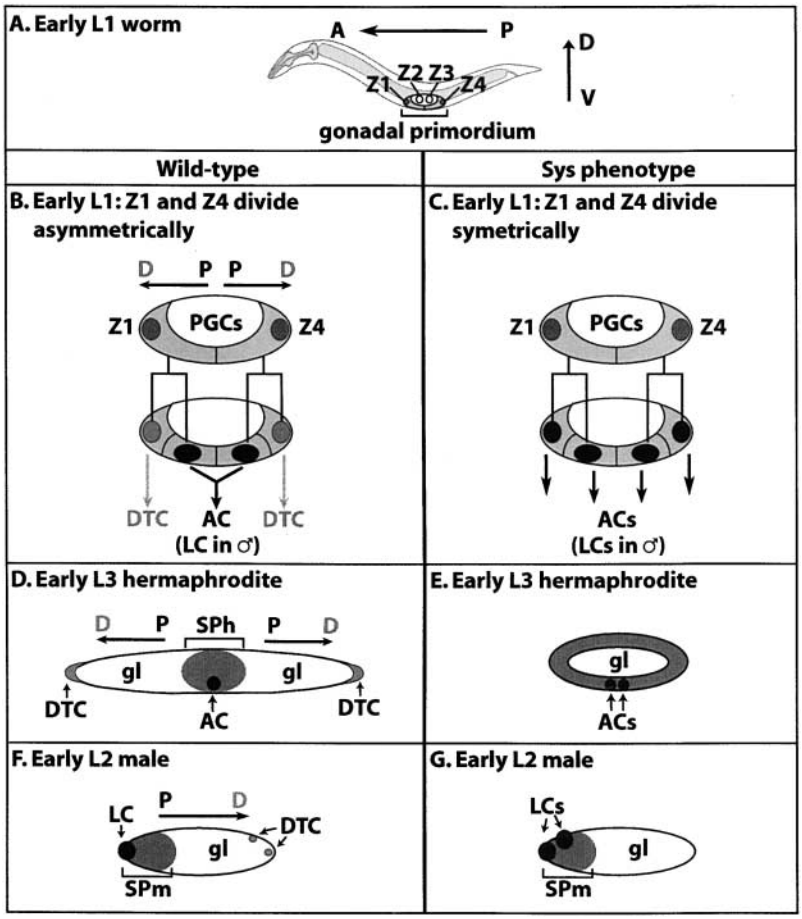

Figure 1.—Early gonad development in wild type and *sys* or Wnt/MAPK mutants. Anterior is to the left and dorsal is to the top. (A, B, D, and F) Wild type. (C, E, and G) Sys defects. (A) A wild-type newly hatched larva showing the anterior-posterior (AP) and dorsal-ventral (DV) body axes. The left-right body axis is not shown. The gonadal primordium consists of the two somatic gonadal precursors, Z1 and Z4, and the two primordial germ cells (PGCs), Z2 and Z3. In the gonadal primordium Z1 and Z4 reside at the anterior and posterior poles of the primordium and reach cytoplasmic processes ventrally (also shown in B, top). The primordial germ cells (PGCs) are central and dorsal to Z1 and Z4. (B) Z1 and Z4 divide asymmetrically in both sexes, each giving rise to a daughter cell with distal identity (gray nucleus) that lies at the poles of the organ, and a daughter cell with proximal identity (black nucleus) that lies more centrally. Each Z1/Z4 distal daughter generates a DTC, while one of the two proximal daughters generates the AC in hermaphrodites and the LC in males. (D) Hermaphrodite somatic primordium (SPh) formation. Most somatic gonadal cells migrate and coalesce centrally (dark gray), separating the germ line (gl) into two separate populations. The distal tip cells (DTCs; light gray) remain at the distal tips of the gonad, leading elongation of the gonadal arms. Each gonadal arm has a proximal-distal (PD) axis. The SPh occupies the proximal-most region of the gonad. (F) Male somatic primordium (SPm). Most somatic gonadal cells (dark gray) occupy the anterior end of the gonad. The germ line (gl) and DTCs lie more posterior. The male gonad has a single proximal-distal axis that coincides with the anterior-posterior axis at this stage in development. (C) The Sys mutant phenotype. Z1 and Z4 divide symmetrically, generating four daughters with proximal identity: all are capable of producing ACs (or LCs in males), but not DTCs. No PD axis is established. (E) In Sys hermaphrodites, somatic gonadal cells (dark gray) do not migrate centrally to form the SPh. Instead, they are arranged around the gonad periphery encasing the germ line (gl). (G) In males, the somatic gonadal cells (dark gray) still cluster anteriorly. However, these males are missing cells with distal fates (the DTCs) and have extra cells with proximal fates (the LCs).

generate one gonadal arm (Kimble and White 1981). The AC is a hermaphrodite-specific cell type and induces vulval development (Kimble 1981). Although each proximal daughter produces a cell with AC potential (or LC potential in males), lateral signaling selects one to adopt the AC (or LC) fate (Greenwald 1998). At the time of AC and LC determination, the DTCs reside at the distal pole(s) while the remaining somatic gonadal blast cells cluster proximally to form the *s*omatic *p*rimordium of *h*ermaphrodites (SPh; Figure 1D) or the *s*omatic *p*rimordium of *m*ales (SPm; Figure 1, D and F).

Establishment of the gonadal PD axis relies on components of the Wnt and MAPK pathways (Sternberg and Horvitz 1988; Siegfried and Kimble 2002). Specifically, the Z1/Z4 asymmetric division is governed by *lin-17*, a homolog of the *frizzled* (*fz*) receptor (Sternberg and Horvitz 1988; Sawa *et al.* 1996), as well as by *wrm-1*/β-catenin, the *pop-1*/TCF transcription factor, and the mitogen-activated protein kinase (MAPK) regulator *lit-1*/*nemo-like kinase* (NLK; Siegfried and Kimble 2002). In addition, the *sys-1* gene (for *s*ymmetrical *s*isters) governs Z1/Z4 polarity (Miskowski *et al.* 2001). Depletion of any one of these regulators can result in a symmetrical Z1/Z4 division, with both daughters adopting a proximal fate. The hallmarks of this fate transformation are a lack of DTCs and generation of extra ACs or LCs (Figure 1, C, E, and F), as well as failure of SPh formation (Figure 1E; Miskowski *et al.* 2001). In males, the SPm forms, but distal cells are sometimes missing and extra LCs are produced, indicating that the PD axis is not specified (Figure 1G; Miskowski *et al.* 2001; Siegfried and Kimble 2002).

Wnt/MAPK signaling also controls asymmetric cell divisions along the AP axis (Herman and Horvitz 1994; Lin *et al.* 1995, 1998; Sawa *et al.* 1996; Kaletta *et al.* 1997; Rocheleau *et al.* 1997, 1999; Thorpe *et al.* 1997; Meneghini *et al.* 1999; Shin *et al.* 1999; Whangbo *et al.* 2000; Herman 2001; Park and Priess 2003). This regulation occurs, at least in part, by controlling the abundance of nuclear POP-1 protein, the *C. elegans* homolog of TCF/LEF1 (Lin *et al.* 1995, 1998; Herman

2001; Maduro *et al.* 2002). Following an anterior-posterior (AP) asymmetric division, the daughter cell with activated Wnt/MAPK signaling has low nuclear POP-1 levels, and its sister has high nuclear POP-1 levels (Lin *et al.* 1995, 1998; Rocheleau *et al.* 1997, 1999; Thorpe *et al.* 1997; Meneghini *et al.* 1999; Shin *et al.* 1999; Herman 2001; Park and Priess 2003). This phenomenon has been dubbed "POP-1 asymmetry" (Maduro *et al.* 2002). Similarly, in Drosophila nuclear Pangolin/TCF is decreased in response to Wnt signaling (Chan and Struhl 2002). Therefore, reduction of nuclear POP-1/TCF may be a conserved mechanism for modulating the ability of this transcription factor to control target genes.

Here we investigate the roles of *sys-1*, several regulators associated with Wnt/MAPK pathways, and four new genes in establishing the PD axis of the gonad. We use a rescuing green fluorescent protein (GFP)::POP-1 transgene to demonstrate that, in the gonad, POP-1 asymmetry reflects the PD axis rather than the AP axis. We also show that *sys-1* is a dose-sensitive locus that interacts genetically with *pop-1* to establish the proximal-distal axis, but that POP-1 asymmetry is not affected in *sys-1* mutants. Finally, we identify *sys-3*, a new locus that, when mutated, has the full complement of Sys defects, genetically interacts with *sys-1* and *pop-1* mutations, and also does not affect POP-1 asymmetry. Mutations in three other genes, *gon-14*, *gon-15*, and *gon-16*, have only some Sys defects, but they also interact genetically with *sys-1* and *pop-1*. Therefore, these *gon* (*gon*adogenesis defective) genes may affect Wnt/MAPK regulation of the gonadal proximal-distal axis, but also have other roles.

MATERIALS AND METHODS

Strains: Animals were grown at 20° unless otherwise noted. All strains were derivatives of Bristol strain N2 (Brenner 1974). The following mutations are described in Hodgkin (1997) or cited references. LG I, *lin-17(n671)*, *pop-1(q645* and *q624)* (Siegfried and Kimble 2002), *mec-8(e398)*, *unc-11(e47)*, *mom-5(or57)* (Thorpe *et al.* 1997), *sys-1(q544)* (Miskowski *et al.* 2001), *lin-6(e1466)*, and *lin-44(n1792)*; LG II, *unc-4(e120)*; LG III, *unc-32(e189)*, *lin-12(n137gf,sd n720lf)*, *unc-119(ed3)*, and *lit-1(or131)* (Meneghini *et al.* 1999); LG IV, *unc-24(e138)*, *unc-33(e204)*, *unc-5(e53)*, *dpy-20(e1282)*, *gon-4(e2575)*, *him-8(e1489)*, and *egl-20(n585)*; and LG V, *rde-1(ne219)* (Tabara *et al.* 1999), *unc-42(e270)*, *sma-1(e30)*, *emo-1(oz1)*, *dpy-11(e224)*, *snb-1(js124)*, and *dpy-13(e184)*; LG X, *mom-1(or10)*, *unc-6(n102)*, and *lon-2 (e678)*. *hT2[qIs48]* and *nT1[qIs51]* were used as dominant green balancer chromosomes (GFP Bal). In addition, the following markers were used: *qIs56* and *qIs57* are *lag-2::GFP* insertions; *syIs50* is a *cdh-3::GFP* insertion; and *qIs65*, *qIs73*, and *qIs74* are GFP::POP-1 insertions.

Construction of POP-1 DNAs: A *pop-1* cDNA was generated by RT-PCR using the Expand High-Fidelity kit (Roche, Indianapolis) with a primer to the SL1 sequence and a primer in the *pop-1* 3′-UTR (5′ CAAAGCATAGAAATAGGCGGG 3′). This cDNA was subcloned using the pT7Blue Perfectly Blunt cloning kit (Novagen) to produce pJK706.

The POP-1::GFP construct (Table 1) included ~3.5 kb of sequence upstream of the *pop-1* gene, introns 1 and 2, and GFP fused at the C terminus of the protein; this construct was produced by a "PCR ligation" technique. First the *pop-1* cDNA::GFP fusion was made by digestion of pJK706 with *Bbs*I, end filling with Klenow, and then digesting with *Hin*dIII to remove the *pop-1* fragment. The GFP vector pPD95.79 was digested with *Hin*dIII and *Sma*I and ligated with the *Hin*dIII *Bbs*I(blunt) fragment from pJK706 to produce plasmid pJK909. The following fragments were then produced either by PCR using the Expand 20Kb^{PLUS} system (Roche) or by digestion and gel purification: (1) a genomic fragment consisting of ~3.5 kb upstream of the start codon and continuing through exon 2 (primer sequences: 5′-AGCAAGGTGTCTACTGTCG CCTGTC-3′ and 5′-TTTTCGCCAATTTTTATGTGT-3′), (2) a genomic fragment containing exon 1 and continuing into exon 3 (primer sequences: 5′-ATGGCCTAACTTCCGC-3′ and 5′-TTTCGCCTGTTCTTCCTTCGA-3′), and (3) a *Pvu*I fragment of pJK909 that begins in exon 3 of the *pop-1 cDNA::GFP* fusion and continues through the *unc-54* 3′-UTR from pPD95.79. These three fragments were produced in duplicate and all were combined and used as the template in PCR reactions to amplify the entire POP-1::GFP product using the Expand 20Kb^{PLUS} system (Roche; primer sequences 5′-AGC AAGGTGTCTACTGTCGCCTGTC-3′ and 5′-GAGGTTTTCA CCGTCATCACC-3′). This construct was expressed in Z1 and Z4 and their descendants as well as other tissues known to express POP-1. However, the GFP did not show different nuclear levels between sister cells in any tissues (Table 1).

Two GFP::POP-1 constructs, GFP::POP-1(Δ1-5) and GFP::POP-1(FL) (Table 1), were made with GFP fused at the N terminus of the *pop-1* cDNA. These reporters were placed under control of a promoter expressed in Z1 and Z4 as well as many other tissues, called *jmp#1* (J. Miskowski, personal communication). GFP::POP-1(Δ1-5) was made by first amplifying GFP with primers containing *Sac*I sites at the 5′ ends. This GFP fragment was cloned in frame into the *Sac*I site of pJK706, which inserts GFP upstream of amino acid 6 of the POP-1 protein. GFP::POP-1(Δ1-5) was subcloned into pPD-49.26 to add the *unc-54* 3′-UTR and then cloned into pDPMM0166 (Maduro and Pilgrim 1995) to add the *unc-119* gene for use as a selective marker when producing transgenics. The resulting plasmid is named pJK789. The second construct, POP-1::GFP(FL), differs from the first only in that GFP is fused in frame upstream of the first methionine of the *pop-1* cDNA. This construct is called pJK908.

Antibody staining, transgenics, and RNAi: Antibody staining on L1 larva was done essentially as described by Herman (2001), using a POP-1 monoclonal antibody (Lin *et al.* 1998), with the following modification: larvae were freeze cracked using two poly-L-lysine-coated slides rather than one slide and one cover slip. We found that staining was inconsistent and extremely weak in the gonad, even though hypodermal tissues stained well. In those animals with detectable POP-1 staining in the gonad, POP-1 was present in Z1 and Z4 and also in Z1/Z4 daughters. In particular, the Z1/Z4 daughters had more nuclear POP-1 staining in proximal than in distal daughters (not shown). Whole-mount techniques using Bouin's fix, collagenase treatment, and Finney-Ruvkin staining gave no visible staining in any tissues.

To produce animals carrying the POP-1::GFP transgene, a mixture of two independently produced POP-1::GFP PCR ligation products (see above) was injected into the distal germ line of *unc-4* animals at 2 ng/μl with 100 ng/μl *unc-4* genomic DNA. One stable transgenic line with weak transmittance of the array was produced, but eventually was lost.

Transgenes of GFP::POP-1(Δ1-5) and GFP::POP-1(FL) were made using particle bombardment as described (Praitis *et al.* 2001) with the following modification: gold beads were baked overnight at 186° before preparing. Plasmid DNA was

prepared using the QIAGEN (Valencia, CA) plasmid midi kit. A total of 640 ng of pJK789 was used per bombardment, producing the insertion *qIs65*, and 780 ng of pJK908 was used per bombardment, producing insertions *qIs72*, *qIs73*, and *qIs74*. These four insertions show similar transgene expression.

RNA interference (RNAi) of *wrm-1* and *lit-1* was performed by injecting 1 mg/ml of dsRNA into *qIs65; unc-32; rde-1* adult hermaphrodites followed by crossing with wild-type males. Injection into *unc-32; rde-1* followed by crossing with wild-type males was always done in parallel. For RNAi of *wrm-1* and *lit-1* in *qIs73* and *qIs74* animals, *unc-32; rde-1* animals were injected with 1 mg/ml of dsRNA followed by crossing with either *qIs73/+* or *qIs74/+* males. Crosses with wild-type males were also done in parallel.

Transgenes containing GFP::POP-1(Δ1-5) and GFP::POP-1 (FL) had some apparent dominant negative activity; however, GFP::POP-1(FL) could rescue gonadogenesis defects in *pop-1 (q624)* animals (Table 1). Animals carrying GFP::POP-1(Δ1-5) often had Sys-like gonadogenesis defects. These defects were not caused by loss of POP-1 asymmetry as all animals had higher POP-1 in the nuclei of proximal Z1/Z4 daughters than in distal Z1/Z4 daughters. GFP::POP-1(Δ1-5) could not be made homozygous in a *sys-3* homozygous mutant background. Because the *qIs65* insertion of GFP::POP-1(Δ1-5) was linked to *sys-1* and *pop-1* it was not crossed into these backgrounds. However, an extrachromosomal array carrying GFP::POP-1 (Δ1-5) with very weak expression did not rescue *pop-1(q645)* mutants and enhanced the gonadogenesis defects in *pop-1 (q624)* mutants. Animals carrying the GFP::POP-1(FL) transgene had no Sys-like gonadogenesis defects. However, animals heterozygous for *sys-1(q544)* and homozygous for *qIs74* were occasionally missing one gonadal arm [gonadal arms are missing at a higher frequency than in *sys-1(q544)* heterozygotes alone]. In addition, the *qIs74* insertion could not be made homozygous in a *sys-3* homozygous background. Despite weak dominant negative activity, *qIs74* could rescue gonadogenesis defects in *pop-1(q624)* mutants, although *pop-1(q645)* mutants were not rescued by this transgene (Table 1).

Identification and characterization of *sys-3*, *gon-14*, *gon-15*, and *gon-16*: The *sys-3*, *gon-14*, *gon-15*, and *gon-16* mutants were isolated in F_2 screens following treatment with ethyl methanesulfonate (EMS); F_2 were raised at 25°. From 8316 mutagenized haploid genomes, we isolated *sys-3(q632)*, *gon-14(q552* and *q631)*, *gon-15(q574)*, and *gon-16(q568)* alleles. The *gon-14(q10*, *q12*, and *q686)* alleles were isolated in other EMS mutagenesis screens (J. Kimble and L. Mathies, unpublished data). All mutations were outcrossed at least five times before further analyses. Males were produced by mating *XX* hermaphrodites with *XO* males. For analysis at 25°, *XO* males raised at 20° were crossed with *XX* hermaphrodites raised at 25°, and crosses were maintained at 25°.

The *sys-3*, *gon-14*, and *gon-16* mutations are all recessive, and the *gon-15* mutation shows minor dominance (Table 8, row 1). We used *nDf32*, which deletes the *gon-14* locus, to ask if *gon-14(q686)* and *gon-14(q631)* are loss-of-function mutations. The hemizygous phenotype of either allele was more severe than its homozygous phenotype. Therefore, these two *gon-14* alleles are likely hypomorphic mutations. There are no existing deficiencies that remove the *sys-3*, *gon-15*, or *gon-16* loci for similar experiments.

For growth assays, synchronized L1's, obtained by bleaching gravid adults and hatching eggs in M9 buffer, were plated on prewarmed 25° plates; larval stages were then scored every 24 hr. Most *sys-3(q632)*, *gon-15(q574)*, and *gon-16(q568)* animals grew at about the same rate as wild-type worms. Most *gon-14(q12)* animals arrested at about the L2 or L3 stage of development. *gon-14(q686)* animals did not arrest, but about half of the animals reached adulthood 24 hr later than wild-type animals.

The four new genes were mapped as follows.

1. *sys-3* resides at +2.8 on LG V: from *sys-3/unc-42 sma-1* animals 3/7 Unc non-Sma carried *sys-3* and 1/2 Sma non-Unc carried *sys-3*; from *sys-3/emo-1 sma-1* animals 11/11 Sma non-Emo carried *sys-3*. The following deficiencies complemented *sys-3(q632)*: *nDf31*, *sDf35*, *sDf29*, and *ctDf1*.
2. *gon-14* resides at +0.1 on LG V: from *gon-14/dpy-11 unc-42* animals 1/22 Dpy non-Unc recombinants carried *gon-14*; from *gon-14/dpy-11 snb-1* animals 2/6 Dpy non-Snb recombinants carried *gon-14*. The deficiency *nDf32* failed to complement *gon-14* mutants.
3. *gon-15* resides at position 0 on LG IV: from *gon-15/dpy-13 unc-24* animals 0/17 Dpy non-Unc carried *gon-15* and 3/3 Unc non-Dpy carried *gon-15*; from *gon-15/unc-33 dpy-13* animals 0/32 Dpy non-Unc recombinants carried *gon-15* and 3/3 Unc non-Dpy carried *gon-15*; from *gon-15/dpy-13 unc-5* animals 0/11 Dpy non-Unc recombinants carried *gon-15* and 15/15 Unc non-Dpy recombinants carried *gon-15*. The following deficiencies complemented *gon-15(q574)*: *mDf10*, *mDf4*, *mDf8*, *mDf9*, and *nDf41*.
4. *gon-16* resides at +3.6 on LG IV: from *gon-16/unc-24 dpy-20* animals 2/29 Unc non-Dpy carried *gon-16* and 19/21 Dpy non-Unc recombinants carried *gon-16*. The following deficiencies complemented *gon-16(q568)*: *eDf19*, *sDf60*, *sDf2*, and *mDf7*. In addition, *gon-16* complemented *gon-3(e2548)*, which maps nearby.

Generation of strains to test double-heterozygous interactions: Animals heterozygous for mutations in both *sys-1* and one other gene were generated in one of five ways. Methods 1–3 used *sys-1(q544)*; methods 4 and 5 used the *sys-1* deficiency *qDf14*: (1) *lin-6 sys-1/hT2[qIs48]* h × *gene-x/GFP Bal* or *gene-x/gene-x* m (strains used for this test were *lin-17/hT2[qIs48]* and *lit-1; him-8*); (2) *gene-x/GFP Bal* or *gene-x/gene-x* h × *lin-6 sys-1/hT2* m (strains used were *dpy-11 sys-3* and *pop-1 mec-8/hT2[qIs48]*); (3) *gene-x/GFP Bal* h × *sys-1/hT2[qIs48]* m (strains used were *pop-1 unc-11/hT2[qIs48]*, *gon-14 unc-42/nT1[unc-?(n754) let-? qIs51]*, *gon-15 unc-5/nT1[qIs51]*); (4) *gene-x/GFP Bal* or *gene-x/gene-x* h × *qDf14/hT2[qIs48]* m (strains used were *pop-1 mec-8/hT2[qIs48]*, *unc-42 sys-3*, *gon-14 unc-42/nT1[qIs51]*, *gon-15 unc-5/nT1[qIs51]*, *unc-24 gon-16/nT1[unc-?(n754) let-? qIs51]*); and (5) *qDf14/hT2[qIs48]* h × *gene-x/GFP Bal* or *gene-x/gene-x* m (strains used were *unc-42 sys-3/nT1[qIs51]*, *lin-17/hT2[qIs48]*, *lit-1; him-8*). For all crosses with *lit-1*, homozygous *lit-1* males were raised at 15° and crosses were done at 20°.

Animals heterozygous for mutations in both *pop-1* and one other gene were generated by crosses similar to those described above for *sys-1*. For all tests except *sys-1* (see above) and *mom-1* (see below) the following cross was done: *gene-x/GFP Bal* or *gene-x/gene-x* h × *pop-1/hT2[qIs48]* m. Strains used were: *sys-3 unc-42*, *gon-14 unc-42/nT1[unc-?(n754) let-? qIs51]*, *gon-15 unc-5/nT1[qIs51]*, and *unc-24 gon-16/nT1[qIs51]*.

Animals heterozygous for mutations in other genes were generated by the following crosses: *sys-3 unc-42* h × *gon-14/nT1 [qIs51]* or *gon-15/nT1[qIs51]* or *gon-16/nT1[qIs51]* m, *gon-15 unc-5/nT1[qIs51]* or *unc-24 gon-16/nT1[qIs51]* h × *gon-14/nT1[qIs51]* m, and *gon-15 unc-5/nT1[qIs51]* h × *unc-24 gon-16/nT1[qIs51]* m.

Because no dominant balancers are available for chromosome *X*, the following crosses were done to generate double heterozygotes with *mom-1*: *mom-1 unc-6/szT1(lon-2)* f (feminized by *fog-1(RNAi)*) × *sys-1/hT2[qIs48]; lon-2/0*, *qDf14/hT2[qIs48]; lon-2/0*, or *pop-1/hT2[qIs48]; lon-2/0* m. Non-Lon, non-*qIs48* progeny were scored for gonadal arms. For all double heterozygotes, control crosses were performed in a similar manner as test crosses. All tests for double heterozygous interactions were done at 20°.

TABLE 1

Summary of POP-1 in the early gonad

Construct name	Reagent description[a]	Expression in Z1/Z4 daughters	Dominant negative?[b]	Rescue?[b]
POP-1::GFP			ND	ND
GFP::POP(Δ1-5)			+++	—
GFP::POP(FL)			+	+

[a] Schematics are drawn to scale, solid boxes are exons; POP-1::GFP carries the *pop-1* 5′ flanking region and the first two introns; the other two use a promoter that expresses GFP in most cells in the animal at the same apparent level.

[b] Rescue of *pop-1(q624)* mutant. See text and MATERIALS AND METHODS for additional details. ND, not determined.

Generation of strains to test dominant enhancement of homozygotes: Dominant enhancement tests were done by segregating *sys-1/+; gene-x/gene-x* from *sys-1/GFP Bal; marker gene-x/+* mothers. As controls, *+/GFP Bal; marker gene-x/marker gene-x* were scored. For example, from *sys-1/hT2[qIs48]; dpy-11 sys-3/+* + hermaphrodites, Dpy Green progeny were scored by differential interference contrast (DIC) optics for number of gonadal arms. This number is compared to the number of gonadal arms scored in Dpy Green animals from *+/hT2 [qIs48]; dpy-11 sys-3/+* + hermaphrodites. All other dominant enhancement tests, except *lin-17*, *lin-44*, and *egl-20*, were done in this way using the following mutant chromosomes: *gon-14 unc-42*, *gon-15 unc-5*, *unc-24 gon-16*, *gon-4 dpy-20*, and *mom-1 unc-6*. To test for dominant enhancement of *lin-17* by *sys-1* the progeny from *lin-17 sys-1/hT2[qIs48]* f (feminized by *fog-1 (RNAi)*) × *lin-17/ hT2[qIs48]* m were compared with the progeny from *lin-17/hT2[qIs48]* f (feminized by *fog-1(RNAi)*) × *lin-17/hT2[qIs48]*. Dominant enhancement of *lin-44* was done in a similar way to *lin-17*. Dominant enhancement of *egl-20* by *sys-1* was done by scoring Glowing progeny from *sys-1/ hT2[qIs48]; egl-20* h. The tests for *pop-1* as a dominant enhancer were done in the same way, with *pop-1* in the place of *sys-1*. All tests for dominant enhancement were done at 20°.

For all genetic interactions null alleles were used when possible. The *mom-1*, *sys-1*, and *pop-1* alleles used are strong loss of function; *lit-1(or131)* is a temperature-sensitive allele known to have gonadal defects when grown at 25°; and the *lin-17*, *lin-44*, and *egl-20* alleles used are null.

RESULTS

The Wnt and MAPK signaling pathways control POP-1 asymmetry to establish the gonadal proximal-distal axes: In many tissues, POP-1 is more abundant in nuclei of anterior than in posterior sister cells after asymmetric divisions along the AP axis (see Introduction). To investigate how POP-1 is regulated in PD divisions in the early gonad, we examined the relative abundance of POP-1 in the nuclei of Z1, Z4, and their daughters. Table 1 summarizes our results.

To examine POP-1 expression, we first used a reporter driven by the *pop-1* promoter, called *pop-1::*GFP (Table 1, MATERIALS AND METHODS), and found GFP in many cells throughout the animal, including Z1, Z4, and their daughters. However, GFP levels were equivalent in the nuclei of Z1/Z4 daughters (Table 1) as well as in anterior and posterior daughters of asymmetric divisions in the hypodermis (not shown). We also attempted to use POP-1 monoclonal antibodies (LIN *et al.* 1998), but staining in the gonad was weak and inconsistent, perhaps due to permeabilization problems (data not shown, see MATERIALS AND METHODS). Nonetheless, in some animals, POP-1 staining was weakly detectable in Z1 and Z4 and their immediate descendants. From these analyses, we conclude that POP-1 is normally present in Z1 and Z4 and their daughters.

During the course of these studies, MADURO *et al.* (2002) reported that GFP fused to the POP-1 N terminus mimicked the asymmetry of endogenous POP-1 in early embryos. We therefore constructed two GFP::POP transgenes under control of a promoter that drives expression at the same apparent level in many cells, including Z1, Z4, and their descendants (J. MISKOWSKI, personal communication; see MATERIALS AND METHODS). One transgene, GFP::POP(Δ1-5), has GFP-coding sequences fused in frame to the sixth codon of *pop-1* cDNA, while the other, GFP::POP(FL), fuses GFP to the full-length *pop-1* cDNA (Table 1). Both transgenes displayed similar expression levels and response to Wnt/MAPK signaling (discussed below). In addition, both transgenes exhibited similar POP-1 asymmetry in the Z1/Z4 daughters (Table 1). GFP::POP(Δ1-5) had dominant negative activity and was not viable in certain mutant backgrounds (Table 1; see MATERIALS AND METHODS); by contrast, GFP::POP(FL) had only marginal dominant negative effects and rescued a *pop-1* mutant (Table 1; see MATERIALS AND METHODS).

We examined both the developing hypodermis and the early gonad using the GFP::POP reporters. As seen

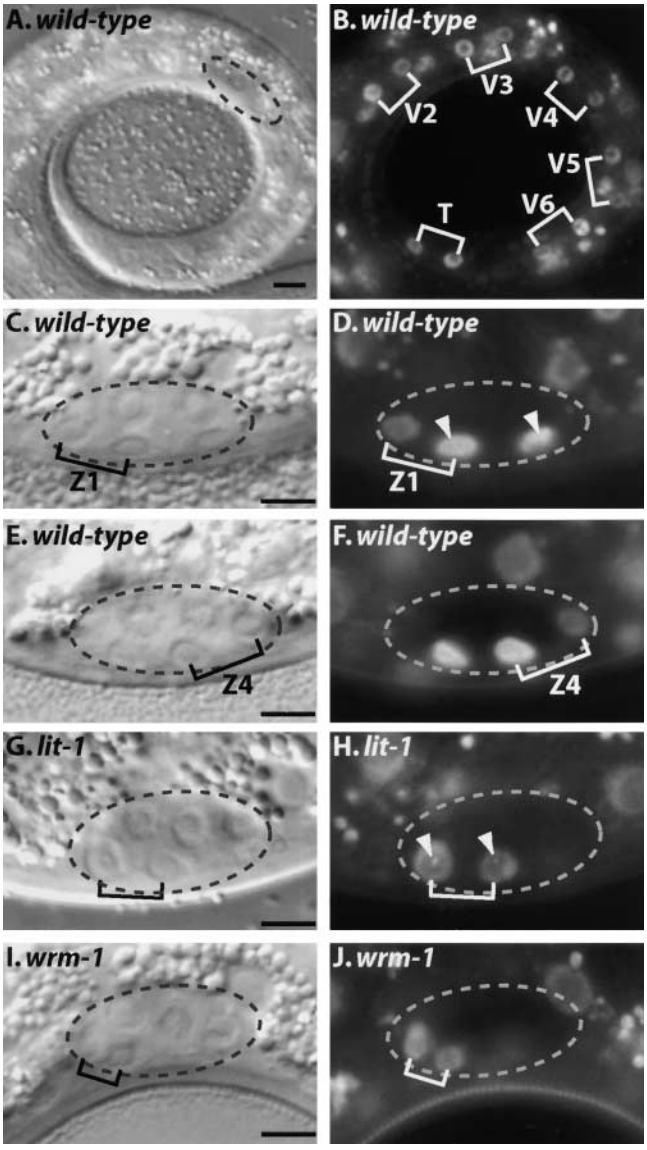

Figure 2.—GFP::POP-1 localization in the Z1/Z4 daughters. All panels show L1 larvae expressing GFP::POP-1(Δ1-5) [animals expressing GFP::POP-1(FL) show similar localization]. The gonad is indicated by the dashed circle. Nuclei of sister cells are indicated by brackets. Images alongside each other are of the same animal: DIC on the left and fluorescence on the right. Bars, 5 μm. (A and B) The T daughters are posterior; (C–J) anterior is to the left. (A and B) In the V and T cell daughters, GFP::POP-1 shows more GFP in nuclei of anterior sister cells than in posterior sister cells. (C–F) GFP::POP-1 is higher in nuclei of the proximal Z1/Z4 daughters than in the distal daughters. GFP-positive puncta are present in the nuclei of the proximal daughters (D, arrowheads). (G–J) *lit-1(RNAi)* or *wrm-1(RNAi)* results in similar nuclear levels of GFP::POP-1 in Z1/Z4 daughters. GFP-positive puncta are often seen in both Z1/Z4 daughters (H, arrowheads). The Z1 daughters are shown.

in previous studies (Lin *et al.* 1998; Herman 2001), GFP was more abundant in anterior than in posterior daughters in hypodermal lineages (Figure 2, A and B). Expression in the early gonad departed from this anterior-posterior asymmetry: the nucleus of Z1.p was brighter than that of Z1.a (Figure 2, C and D), and the nucleus of Z4.a was brighter than that of Z4.p (Figure 2, E and F). We also noted that proximal daughters contained nuclear GFP puncta (Figure 2D, arrowheads) similar to those described in the anterior daughters of asymmetric divisions in the embryo (Maduro *et al.* 2002). We conclude that, in the gonad, the proximal daughters of Z1 and Z4 have more nuclear GFP::POP-1 than do the distal daughters, reflecting the proximal-distal axis of the gonad rather than the anterior-posterior axis of the animal.

To investigate the effect of Wnt/MAPK pathways on POP-1 asymmetry in the gonad, we used RNAi or mutants to block regulation of Wnt or MAPK signaling in GFP::POP transgenic animals. POP-1 asymmetry was lost in the early gonad using either *wrm-1(RNAi)* or *lit-1(RNAi)*: Z1 and Z4 daughters displayed apparently equivalent levels of nuclear POP-1 when either of these two genes was reduced (Figure 2, G–J). In this experiment, we assessed the relative level of POP-1::GFP between sister cells in the same animal, rather than the absolute level. Although the level in both mutant nuclei can appear somewhat lower than that of the wild-type proximal sister, GFP puncta are often observed in both mutant daughters (Figure 2H, arrowheads). In wild type, these puncta are observed in nuclei with high nuclear GFP::POP-1. Additionally, *lin-17(n671)* animals displayed equivalent levels of nuclear POP-1 in 31% of Z1 and Z4 daughters (data not shown). This penetrance is consistent with the penetrance of distal to proximal transformations in this mutant (Sternberg and Horvitz 1988; Siegfried and Kimble 2002). Therefore, the asymmetry exhibited by GFP::POP(Δ1-5) and GFP::POP(FL) in the daughters of Z1 and Z4 is regulated by Wnt/MAPK signaling.

***sys-1* interacts genetically with *pop-1* and *lin-17* to control Z1/Z4 asymmetry:** The proximal-distal axis of the gonad is affected similarly in Wnt/MAPK and *sys-1* mutants (Sternberg and Horvitz 1988; Miskowski *et al.* 2001; Siegfried and Kimble 2002). This similarity suggested that *sys-1* might influence Wnt and/or MAPK signaling. To explore this hypothesis, we analyzed genetic interactions between *sys-1* and Wnt/MAPK genes. First, we assayed double heterozygotes, which are animals heterozygous for mutations in both *sys-1* and one of the Wnt/MAPK genes. This classic test for nonallelic noncomplementation asks if animals of the genotype *gene-x/+; gene-y/+* have more severe defects than that predicted for the additive effect of each heterozygote individually. Second, we assayed animals heterozygous for *sys-1,* but homozygous for a second mutation. This test, for dominant enhancement of homozygous mutants, is more sensitive than that relying on double heterozygotes. Our results are summarized in Table 2 and detailed in Tables 3 and 4.

We first focused on genetic interactions between *sys-1*

TABLE 2

Summary of genetic interactions

	Double heterozygotes:	Dominant enhancement	
gene-x	*sys-1*/+; *gene-x*/+	*sys-1*/+; *gene-x*/*gene-x*	*pop-1*/+; *gene-x*/*gene-x*
Wnt/MAPK genes			
pop-1	+	ND	NA
lin-17	−	+	ND
lit-1	−	ND	ND
mom-1	−	−	−
egl-20	ND	−	−
lin-44	ND	−	ND
sys			
sys-3	+	+	+
gon genes			
gon-14	−	+	+
gon-15	−	+	+
gon-16	−	+	+
gon-4	ND	−	−

For actual data see Tables 3, 4, 8, and 9; +, interaction observed; −, no interaction; ND, not determined; NA, not applicable.

and *pop-1*. Hermaphrodites homozygous for either *sys-1 (q544)* or *pop-1(q645)* have a fully penetrant loss of DTCs, representing complete loss of the distal fate (Miskowski *et al.* 2001; Siegfried and Kimble 2002); furthermore, both mutations are essentially recessive: DTCs were missing in ≤1% of *sys-1(q544)*/+ and *pop-1(q645)*/+ single heterozygotes (Table 3). The *pop-1(q624)* mutation is fully recessive (Siegfried and Kimble 2002) and a deficiency that deletes *sys-1*, *qDf14*, has mild haplo-insufficiency (2%, Table 3). A marked genetic interaction was seen between *sys-1* and *pop-1*: + *sys-1(q544)*/*pop-1 (q645)* + double heterozygotes resulted in a 21% loss of DTCs (Table 3), + *sys-1(q544)*/*pop-1(q624)* + were missing 15% of their DTCs ($n = 68$), and *qDf14 in trans* to *pop-1(q645)* had a 55% DTC loss (Table 3). A deletion internal to the *sys-1* locus had the same effect as *qDf14* in this assay (A. Kidd and K. Siegfried, unpublished results), suggesting that *qDf14* represents the effect of a *sys-1* null. We conclude that *sys-1* and *pop-1* interact genetically and that *sys-1* is a dose-sensitive gene.

We next asked if *sys-1* interacted with other Wnt/MAPK genes, focusing on genes with known Sys-like gonadogenesis defects: *mom-1/porcupine* (*porc*), *lin-17/fz*, and *lit-1/NLK* (Sternberg and Horvitz 1988; Siegfried and Kimble 2002). We found that, as double heterozygotes, none had a significant interaction with *sys-1* (Tables 2 and 3). We therefore used the more sensitive test of dominant enhancement. Specifically, we asked if *sys-1* could dominantly enhance *mom-1/porc*, *egl-20*/Wnt, *lin-44*/Wnt, or *lin-17/fz* homozygotes (*lit-1* could not be tested due to balancer constraints) and if *pop-1* could dominantly enhance *mom-1* or *egl-20* mutants (dominant enhancement of *lin-17* by *pop-1* was not tested because these genes are closely linked; Tables 2 and 4). Only one interaction was found: whereas *lin-17* homozygotes had 12% DTC loss, *lin-17 sys-1*/*lin-17* + mutants had 29% DTC loss (Table 4). We conclude that *sys-1* interacts genetically with both *pop-1* and *lin-17*. However, the interaction between *sys-1* and *pop-1* is substantially stronger than that between *sys-1* and *lin-17*.

Identification of additional genes regulating Z1 and Z4: To identify other genes controlling Z1/Z4 asymmetry, we screened for mutants with a Sys-like phenotype (see materials and methods). The initial screen focused on mutants that lacked gonadal arm elongation

TABLE 3

Double heterozygotes of *sys-1* and Wnt/MAPK mutants

	gene-y				
gene-x	+/+	*mom-1*/+	*lin-17*/+	*lit-1*/+	*pop-1*/+
+/+	0 $n > 200$	0 $n = 198$	0 $n = 132$	0 $n = 206$	1 $n = 154$
sys-1					
q544/+	<1 $n = 508$	1 $n = 188$	0 $n = 170$	0 $n = 212$	21 $n = 120$
qDf14/+	2 $n = 426$	3 $n = 160$	4 $n = 170$	4 $n = 238$	55 $n = 202$
pop-1/+	1 $n = 154$	0 $n = 98$	ND	ND	NA

Values are percentage of DTCs missing, assayed by gonadal arm elongation. n, number of arms scored. Alleles used are *sys-1(q544)*, *mom-1(or10)*, *lin-17(n671)*, *lit-1(or131)*, and *pop-1 (q645)*. Data for *pop-1* interactions are significant with $P < 0.0001$. ND, not determined; NA, not applicable.

TABLE 4

sys-1* is a dominant enhancer of *lin-17/fz

	gene-y				
gene-x	+/+	*mom-1/mom-1*	*egl-20/egl-20*	*lin-44/lin-44*	*lin-17/lin-17*
+/+ or Bal[a]	ND	0 n = 202	0 n = 124	0 n = 110	12 n = 144
sys-1/Bal	0 n = 202	0 n = 228	1 n = 160	0 n = 78	29 n = 180
pop-1/Bal	<1 n = 208	1 n = 185	0 n = 160	ND	ND

Values are percentages of DTCs missing, assayed by gonadal arm elongation. n, number of arms scored. Alleles used are *mom-1(or10)*, *egl-20(n585)*, *lin-44(n1792)*, and *lin-17(n671)*. The interaction between *lin-17* and *sys-1* is significant with $P < 0.0001$.

[a] See MATERIALS AND METHODS for genotype used in each mutant background.

and failed to make an SPh, two features typical of *sys-1*. Five additional genes were identified in this screen: *pop-1* (SIEGFRIED and KIMBLE 2002), *sys-3*, *gon-14*, *gon-15*, and *gon-16* (see MATERIALS AND METHODS). The *gon-14* locus is represented by five alleles, and *sys-3*, *gon-15*, and *gon-16* are each represented by a single allele. None of these loci mapped genetically to positions that encode known Wnt/MAPK components (Figure 3).

To learn if the newly identified genes affected Z1/Z4 asymmetry, we scored mutations in each for loss of DTCs, which mark the distal fate, and extra ACs, which mark the proximal fate. To score DTCs, we used the *lag-2::GFP* reporter (Figure 4, A and D; BLELLOCH *et al.* 1999), and to score ACs, we used *cdh-3::GFP* (PETTITT *et al.* 1996). As expected, *sys-3*, *gon-14*, *gon-15*, and *gon-16* mutants failed to make DTCs (Table 5; Figure 4, B and E), but DTC loss was not fully penetrant and was temperature sensitive (Table 5). Analysis of AC formation gave an unexpected result. Whereas most *sys-1* and *pop-1* mutants made two or more ACs, as described previously (MISKOWSKI *et al.* 2001; SIEGFRIED and KIMBLE 2002), most *sys-3*, *gon-15*, *gon-16*, and many *gon-14* mutants had only one AC, although a few had more (Table 6). We next asked if the percentage of animals with extra ACs could be enhanced by removal of *lin-12* activity. The rationale for this experiment was as follows. Normally, only one of two potential AC precursors adopts the AC fate due to lateral signaling mediated by the *lin-12*/Notch receptor; however, in *lin-12* mutants, both AC precursors adopt the AC fate (GREENWALD 1998). Therefore, our assay for AC production might underestimate the production of extra proximal cells. We examined all four mutants in a *lin-12(0)* background so that all Z1/Z4 daughters with proximal fate could give rise to ACs. The extra AC defect was dramatically enhanced in *sys-1* and *pop-1* mutants as well as in *sys-3* mutants (Table 6). We conclude that the *sys-3* locus affects Z1/Z4 asymmetry.

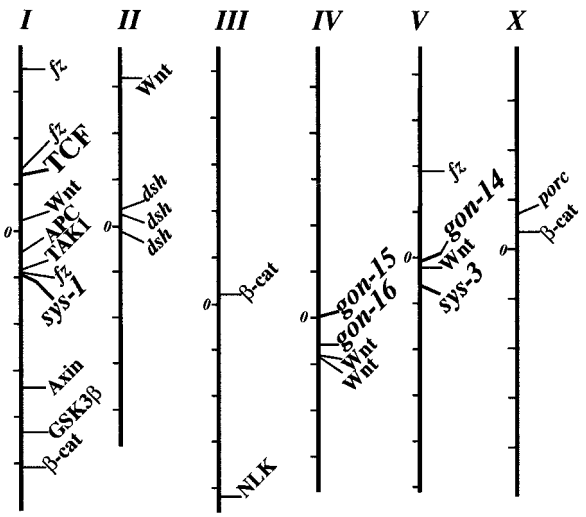

FIGURE 3.—The *sys-3*, *gon-14*, *gon-15*, and *gon-16* genes do not map to Wnt/MAPK signaling components. Approximate genetic map location of canonical Wnt pathway components and MAPK members that regulate Wnt signaling are shown. Linkage groups (LG) are designated by Roman numerals and *X* for the sex chromosome. Corresponding *C. elegans* gene names are as follows, from LG I left (top) to LG X right (bottom): *mig-1/fz*, *lin-17/fz*, *pop-1*/TCF, *lin-44*/Wnt, *apr-1*/APC, *mom-4*/TAK1, *mom-5/fz*, *pry-1*/Axin, *sgg-1*/GSK3β, *hmp-2*/β-catenin, *cwn-1*/Wnt, C27A2.6/*dsh*, C34F11.9/*dsh*, *mig-5/dsh*, *wrm-1*/β-catenin, *lit-1*/NLK, *egl-20*/Wnt, *cwn-2*/Wnt, *cfz-2/fz*, *mom-2*/Wnt, *mom-1/porc*, and *bar-1*/β-catenin. Although *sys-1* mapped near *mom-5/fz*, mutations in these two genes complemented each other, and a deficiency distinguished the two loci: *qDf14* removed *sys-1*, but not *mom-5*.

For *gon-14*, *gon-15*, or *gon-16*, the percentage of animals with extra ACs was not enhanced by reduction of *lin-12* activity (Table 6). The apparent loss of ACs in *gon-14*, *gon-15*, or *gon-16* mutants, in either a *lin-12*(+) or a *lin-12(0)* background, may be caused by production of fewer than normal AC precursors, defects in AC specification, or defects in AC maintenance. An exploration of the loss of ACs in these mutants is beyond the scope of this work.

While scoring *gon-14*, *gon-15*, and *gon-16* mutants for DTC loss and extra ACs, we noticed additional gonado-

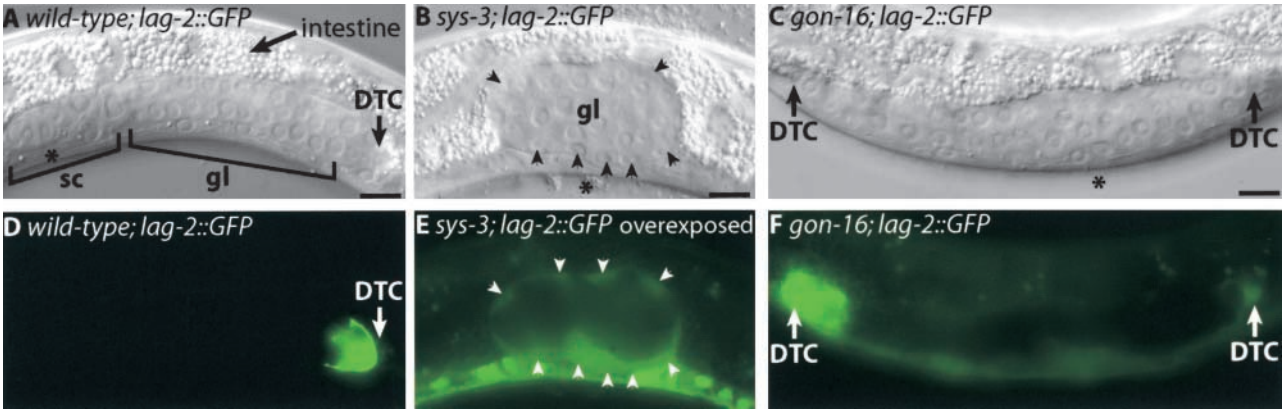

FIGURE 4.—Gonadogenesis defects of *sys-3*, *gon-14*, *gon-15*, and *gon-16*. (A–F) L3 hermaphrodites; (A–C) DIC; (D–F) fluorescence; asterisk, center of animal; DTC, distal tip cell; sc, somatic cells. Bars, 10 μm. (A and D) Wild-type posterior gonad. The somatic gonadal cells (sc) are clustered centrally. The elongating germ line (gl) is led by the DTC, which expresses *lag-2::GFP*. (B and E) *sys-3* mutant, the entire gonad is shown. The gonad is not elongated and no *lag-2::GFP*-expressing DTCs are seen. Residual *lag-2::GFP* is present in all somatic gonadal cells upon overexposure (arrowheads). Somatic gonadal cells (arrowheads) are arranged around the periphery of the gonad surrounding the germ line (gl). Cells expressing GFP ventral to the gonad are cells in the ventral nerve cord. (C and F) The *gon-16* mutant can have weakly expressing DTCs. The anterior DTC has normal *lag-2::GFP* expression, while the posterior DTC has very weak expression. A similar phenomenon is seen in *gon-14* and *gon-15* mutants.

genesis defects. For example, DTCs often migrated more slowly than normal, and gonadal arms could be unusually short. In addition, the DTC expression of *lag-2::GFP* was often lower than normal (Figure 4F), and AC expression of *cdh-3::GFP* was often abnormally weak or not detectable. On the basis of the reduced DTC function and the poor DTC and AC reporter expression, we suggest that DTCs and ACs may not develop properly in *gon-14*, *gon-15*, and *gon-16* mutants.

***sys-3*, *gon-14*, *gon-15*, and *gon-16* function in male gonadogenesis:** To ask if the *sys-3*, *gon-14*, *gon-15*, and *gon-16* mutants have similar gonadogenesis defects in males as in hermaphrodites, we compared DTC production in the two sexes. To detect DTCs in males, we used a functional assay. Normally, male DTCs are essential for germ-line proliferation: males with no DTCs have only a few germ cells, a defect called Glp (*g*erm-*l*ine *p*roliferation defective; KIMBLE and WHITE 1981). We compared

TABLE 5

***sys*, *pop*, and *gon* effects on hermaphrodite DTC and T cells**

		% animals with *x* DTCs[a]				T cell defects[b]	
Genotype	Temperature	2	1	0	*n*	%	*n*
Wild type	20°	93	7	0	108	0	96
Wild type	25°	98	2	0	56	1	128
sys-1(q544)[c]	20°	0	0	100	40	5	112
pop-1(q645)[d]	20°	0	0	100	>100	40	86
sys-3(q632)	20°	42	46	12	102	0	98
sys-3(q632)	25°	24	33	43	106	4	116
gon-14(q686)	20°	100	0	0	54	ND	
gon-14(q686)	25°	3	38	59	99	16	126
gon-15(q574)	20°	86	14	0	57	ND	
gon-15(q574)	25°	31	44	25	96	1	82
gon-16(q568)	20°	86	12	2	49	ND	
gon-16(q568)	25°	40	40	20	124	5	88

sys-3 and *gon-14* homozygotes were derived from homozygous *sys-3* and *gon-14* parents, respectively. *sys-1*, *pop-1*, *gon-15*, and *gon-16* were derived from heterozygous parents.

[a] Assayed using *lag-2::GFP*. *qIs56* was used for wild type, *pop-1*, *gon-15*, and *gon-16*; *qIs57* was used for *sys-3* and *gon-14*.

[b] Percentage of phasmids that do not fill with dye.

[c] Data for *sys-1* DTCs are from MISKOWSKI *et al.* (2001).

[d] All *pop-1* data are from SIEGFRIED and KIMBLE (2002).

TABLE 6

***sys*, *pop*, and *gon* effects on anchor cells**

		% animals with *x* ACs: *lin-12(+)*[a]					% animals with *x* ACs: *lin-12(0)*[a]				
Genotype	Temperature	0	1	2	≥3[c]	*n*	0	1	2	≥3[d]	*n*
Wild type	20°	0	100	0	0	45	0	6	91	3	35
Wild type	25°	0	98	2	0	63	0	6	74	21	34
sys-1(q544)	20°	0	4	70	26	27	0	0	0	100	27
pop-1(q645)[b]	20°	0	14	70	16	44	0	0	0	100	24
sys-3(q632)[e]	20°	0	97	3	0	59	0	4	61	35	23
sys-3(q632)[e]	25°	2	90	8	0	62	ND	ND	ND	ND	
gon-14(q686)[e]	25°	45	40	11	4	47	47	33	17	3	30
gon-15(q574)[f]	25°	29	65	6	0	49	4	74	19	4	27
gon-16(q568)[f]	25°	9	86	5	0	56	0	70	26	4	27

[a] Assayed using the *cdh-3::GFP* insertion *syIs50*.
[b] All *pop-1* data are from Siegfried and Kimble (2002).
[c] Percentage of animals with *x* number of ACs: *sys-1* 3AC (15%), 4AC (7%), ≥5AC (4%); *gon-14* 3AC (2%), 4AC (2%).
[d] Percentage of animals with *x* number of ACs: wild type 20° 3AC (3%); wild type 25° 3AC (15%), 4AC (6%); *sys-1* 3AC (19%), 4AC (11%), ≥5AC (70%); *sys-3* 3AC (26%), 4AC (9%); *gon-14* 3AC (0%), 4AC (3%); *gon-15* 3AC (4%); *gon-16* 3AC (4%).
[e] *sys-3* and *gon-14* homozygotes derived from homozygous *sys-3* and *gon-14* parents, respectively.
[f] *sys-1*, *pop-1*, *gon-15*, and *gon-16* were derived from heterozygous parents.

the percentage of hermaphrodites missing both DTCs (using *lag-2::GFP*) to the percentage of Glp males (Table 7). By these assays, *gon-14*, *gon-15*, and *gon-16* mutant hermaphrodites apparently lacked DTCs somewhat more often than did mutant males (Table 7). This result is similar to that observed for *sys-1* and *pop-1* (Miskowski *et al.* 2001; Siegfried and Kimble 2002). By contrast, 93% of *sys-3* males lacked both DTCs, whereas only 12% of *sys-3* hermaphrodites were missing both DTCs (Table 7). Therefore, *sys-1*, *pop-1*, *gon-14*, *gon-15*, and *gon-16* appear to be more critical for hermaphrodite gonadogenesis, while *sys-3* appears to be more important for male gonadogenesis.

In addition to the Glp phenotype, *gon-14*, *gon-15*, and *gon-16* mutant males often had disorganized gonads with elongation defects and *gon-14(q686)* mutant males occasionally produced a vulva (6%, $n = 47$, 25°). No defect in elongation was detected in *sys-3* male gonads, but somatic gonadal tissues were sometimes positioned abnormally within the gonad, as has been seen in *sys-1* and *pop-1* males (K. Siegfried, unpublished observation). The elongation defects in both hermaphrodite and male gonads suggest that *gon-14*, *gon-15*, and *gon-16* affect leader cell function.

T cell polarity and other nongonadal defects: To ask if *sys-1*, *sys-3*, *gon-14*, *gon-15*, and *gon-16* were gonad specific, we assayed each for a role in nongonadal development. We first examined their growth rate and found that all mutants except *gon-14* progressed through larval development at a rate similar to wild-type animals (see materials and methods). For *gon-14*, most animals homozygous for the strong loss-of-function allele *gon-14 (q12)* arrested at midlarval development (L2 or L3), but animals homozygous for the temperature-sensitive allele, *gon-14(q686)*, developed to adulthood more slowly than wild type (see materials and methods). In addition, whereas *sys-3* mutant adults attained a normal size, *gon-14*, *gon-15*, and *gon-16* adults were typically about one-half to two-thirds the length of wild-type adults. Therefore, *gon-14*, *gon-15*, and *gon-16* all affect growth and therefore are unlikely to act specifically in gonadogenesis.

We next asked if *sys-3*, *gon-14*, *gon-15*, or *gon-16* acts in other Wnt/MAPK-dependent cell fate decisions. To do this, we examined production of functional phasmid socket cells by the T cell, a precursor in the tail hypodermis. Normally, the posterior T cell daughter gives rise to the phasmid socket cells, while its anterior daughter makes primarily hypodermis (Sulston and Horvitz 1977). Wnt/MAPK signaling controls this asymmetric T cell division: abrogation of Wnt/MAPK signaling causes either a reversal of cell polarity or both daughters to adopt an anterior identity (Herman and Horvitz 1994; Sawa *et al.* 1996; Rocheleau *et al.* 1999; Herman 2001). We assayed for the production of phasmid socket cells, using a dye-filling assay (Herman and Horvitz 1994). The *sys-1*, *sys-3*, *gon-15*, and *gon-16* mutants had little effect on phasmid socket cells, but the *gon-14(q686)* temperature-sensitive mutant raised at restrictive temperature sometimes failed to take up dye into the phasmids (Table 5). The *gon-14* effect on phasmid socket cells may reflect a lack of socket cells due to a lineage defect or a failure of socket cells to function properly.

Finally, *gon-15* and *gon-16* males raised at 25° were often missing some or all sensory rays (data not shown), a phenotype seen in *lin-17* mutants, in *pop-1(RNAi)* ani-

TABLE 7

Comparison of *sys*, *pop*, and *gon* hermaphrodite and male defects

		⚥ with both DTCs missing[a]		♂ Glp[b]	
Genotype	Temperature	% no DTC	*n*	% Glp	*n*
Wild type	20°	0	108	0	107
Wild type	25°	0	56	3	111
sys-1(q544)[c]	20°	100	40	19	62
pop-1(q645)[d]	20°	100	>100	5	105
sys-3(q632)	20°	12	102	93	43
gon-14(q686)	25°	59	99	28	47
gon-15(q574)	25°	26	96	17	24
gon-16(q568)	25°	20	124	8	25

[a] Assayed with *lag-2::GFP* (*qIs56* for *pop-1*, *gon-15*, and *gon-16* and *qIs57* for *sys-3* and *gon-14*).
[b] Scored for lack of germ-line proliferation by DIC optics.
[c] Data for *sys-1* hermaphrodite DTCs are from Miskowski *et al.* (2001).
[d] All *pop-1* data are from Siegfried and Kimble (2002).

mals, and occasionally in *sys-1* mutants (Sternberg and Horvitz 1988; Siegfried and Kimble 2002; this work). No obvious male tail defects were observed in *gon-14 (q686)* mutants raised at 25° or in *sys-3* mutant males raised at 20°.

Genetic interactions among *sys-1*, *pop-1*, *sys-3*, *gon-14*, *gon-15*, and *gon-16*: The genetic interactions observed between *sys-1* and components of the Wnt pathway (Table 2) provided a sensitive assay for gene function in Z1/Z4 asymmetry (see above). We therefore asked whether *sys-3*, *gon-14*, *gon-15*, and *gon-16* might interact genetically with either *sys-1* or *pop-1*. First, we looked for interactions between double heterozygotes and found that *sys-3* did indeed interact with *sys-1* in this test, but no other interactions were observed (Tables 2 and 8). This result provides further support for a role of *sys-3* in Z1/Z4 asymmetry.

As a more sensitive assay for genetic interactions, we next asked if *sys-1* or *pop-1* could dominantly enhance *sys-3*, *gon-14*, *gon-15*, or *gon-16* mutants. Intriguingly, either *sys-1/+* or *pop-1/+* enhanced the 20° phenotype of each of these mutants (Tables 2 and 9). As a control, we tested *gon-4* for dominant genetic interactions with *sys-1* and *pop-1*. In *gon-4* mutants, cell divisions are severely delayed during gonadogenesis, and DTCs and ACs are often missing (Friedman *et al.* 2000). Therefore, *gon-4* mutants have defects in gonadogenesis that are distinct from those in the mutants under study here, but sufficiently similar to serve as a reasonable control. We observed no dominant enhancement of *gon-4* by either *sys-1/+* or *pop-1/+* (Tables 5 and 9). Therefore, genetic interactions between *sys-1* or *pop-1* and *sys-3*, *gon-14*, *gon-15*, or *gon-16* appear to be specific.

***sys-1*, *sys-3*, *gon-14*, *gon-15*, and *gon-16* do not regulate POP-1 asymmetry:** Wnt/MAPK regulators control POP-1 asymmetry in Z1 and Z4 daughters, as assayed by our GFP::POP-1 reporter (see above, Figure 2). To investigate how *sys-1*, *sys-3*, *gon-14*, *gon-15*, and *gon-16* cooperate with Wnt/MAPK regulators, we assayed GFP::POP-1 localization in these mutants. In contrast to the Wnt/MAPK mutants, which eliminate POP-1 asymmetry, *sys-1*, *sys-3*, *gon-14*, *gon-15*, and *gon-16* mutants did not affect POP-1 asymmetry (Figure 5). Therefore, these genes are likely to function either downstream of or in parallel to the regulation of POP-1 asymmetry by Wnt and MAPK signaling.

DISCUSSION

In this work, we investigate the control of the asymmetric division of Z1 and Z4 that sets up the PD axis during early gonadogenesis. Previous work showed that the *sys-1* gene and Wnt/MAPK regulators were critical for this asymmetric division (Sternberg and Horvitz 1988; Miskowski *et al.* 2001; Siegfried and Kimble 2002). Here we explore the subcellular localization of POP-1 in Z1/Z4 daughters and its regulation by Wnt/MAPK regulators. We also report that *sys-1* is a dose-sensitive locus that interacts genetically with Wnt signaling regulators as well as a group of four newly identified genes affecting early gonadogenesis. The new genes include *sys-3*, which controls Z1/Z4 asymmetry, and *gon-14*, *gon-15*, and *gon-16*, which control development more broadly.

POP-1 asymmetry in the gonad reflects the proximal-distal axis: The POP-1 transcription factor is required for proximal-distal fate specification among the Z1/Z4 daughters (Siegfried and Kimble 2002). By contrast, in several nongonadal tissues, POP-1 controls sister cell fates along the AP body axis (Herman and Horvitz 1994; Lin *et al.* 1995, 1998; Sawa *et al.* 1996; Kaletta *et al.* 1997; Rocheleau *et al.* 1997, 1999; Thorpe *et al.* 1997; Meneghini *et al.* 1999; Shin *et al.* 1999; Whangbo *et al.* 2000; Herman 2001; Park and Priess 2003). In AP asymmetric divisions, POP-1 is more abundant in anterior nuclei than in posterior nuclei (Lin *et al.* 1995,

TABLE 8

Tests for genetic interactions in double heterozygotes

	gene-y						
	sys-1						
gene-x	*q544/+*	*qDf14/+*	*pop-1/+*	*sys-3/+*	*gon-14/+*	*gon-15/+*	*gon-16/+*
+/+	<1 n = 508	2 n = 426	1 n = 154	0 n = 170	0 n = 160	1 n = 276	0 n = 398
sys-1							
q544/+		100 n = 92	21 n = 152	3 n = 292	0 n = 144	0 n = 104	0 n = 158
qDf14/+			55 n = 202	15 n = 196	1 n = 190	3 n = 180	2 n = 164
pop-1/+				1 n = 154	0 n = 180	0 n = 154	0 n = 170
sys-3/+					0 n = 166	0 n = 194	0 n = 200
gon-14/+						0 n = 140	0 n = 154
gon-15/+							0 n = 146

Values are percentage of DTCs missing, assayed by gonadal elongation. n, number of arms scored. For *sys-1*, both *sys-1(q544)* and the *qDf14* deficiency were used. Other alleles were *pop-1(q645)*, *sys-3(q632)*, *gon-14(q631)*, *gon-15(q574)*, and *gon-16(q568)*. The interaction between *qDf14* and *sys-3* is significant with $P < 0.0001$.

1998; Rocheleau *et al.* 1997, 1999; Thorpe *et al.* 1997; Meneghini *et al.* 1999; Shin *et al.* 1999; Herman 2001; Park and Priess 2003), a phenomenon dubbed POP-1 asymmetry (Maduro *et al.* 2002). To ask if POP-1 asymmetry is seen in Z1/Z4 daughters, we used reporter transgenes to assay POP-1 localization. We found that POP-1 is indeed asymmetric in Z1/Z4 daughters, but that this asymmetry did not follow the AP axis. Instead POP-1 asymmetry in the early gonad reflects the PD axis. Thus, distal nuclei (Z1.a and Z4.p) have less nuclear POP-1, and proximal nuclei (Z1.p and Z4.a) have more nuclear POP-1.

The POP-1 asymmetry in Z1/Z4 daughters is controlled by Wnt/MAPK regulators. We have shown that *lin-17/frizzled*, *wrm-1*/β-catenin, and *lit-1*/NLK each regulate POP-1 asymmetry in these cells. These same regulators control distal fates in the early gonad (Sternberg and Horvitz 1988; Siegfried and Kimble 2002). Therefore, Wnt/MAPK regulators are likely to control both POP-1 asymmetry and POP-1 activity.

How do Wnt/MAPK regulators control anterior-posterior asymmetries in the main body and proximal-distal asymmetries in the gonad? We suggest three possibilities. One idea is that POP-1 is activated by different ligands in the two situations. Three of the five Wnt homologs have been identified as critical for AP divisions: *mom-2*, *lin-44*, and *egl-20* (Herman and Horvitz 1994; Rocheleau *et al.* 1997; Thorpe *et al.* 1997; Whangbo *et al.*

TABLE 9

Dominant enhancement by *sys-1* and *pop-1*

	gene-y					
gene-x	+/+	*sys-3/sys-3*	*gon-14/gon-14*	*gon-15/gon-15*	*gon-16/gon-16*	*gon-4/gon-4*
+/*Bal*	ND	48 n = 122	24 n = 136	8 n = 136	5 n = 182	36 n = 220
sys-1/Bal	0 n = 202	83 n = 136	83 n = 126	30 n = 162	19 n = 156	31 n = 200
pop-1/Bal	<1 n = 208	87 n = 136	70 n = 128	44 n = 148	34 n = 172	40 n = 210

Values are percentage of DTCs missing, assayed by gonadal arm elongation. n, number of arms scored. Alleles were *pop-1(q645)*, *sys-1(q544)*, *sys-3(q632)*, *gon-14(q631)*, *gon-15(q574)*, *gon-16(q568)*, and *gon-4(e2575)*. All genetic interactions observed are significant with $P < 0.0001$. For *gon-4 sys-1* and *gon-4 pop-1* no significant interaction was observed; $P = 0.16$ and $P = 0.43$, respectively.

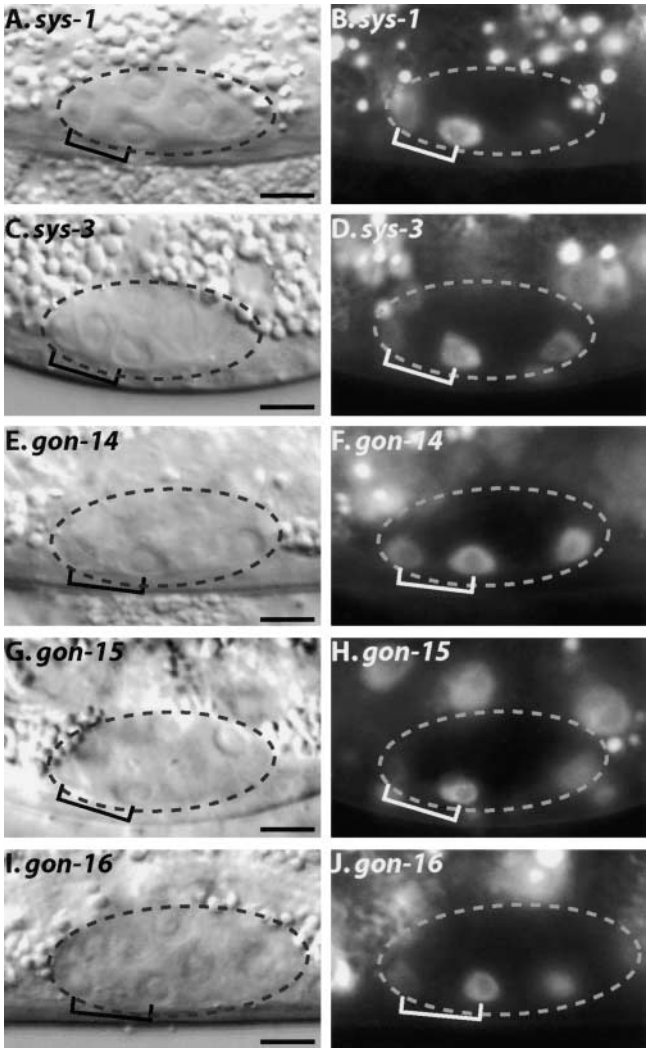

Figure 5.—GFP::POP-1 in *sys* and *gon* mutants. The *sys-1*, *sys-3*, *gon-14*, *gon-15*, and *gon-16* mutants are not required for GFP::POP-1 asymmetry in the gonad. The gonad is indicated by the dashed circle. Nuclei of Z1 daughters are shown (brackets). Images alongside each other are of the same animal: DIC on the right and fluorescence on the left. Bars, 5 μm. (A–J) All mutants have normal POP-1 nuclear asymmetry (compare to Figure 2, C and D); proximal Z1/Z4 daughters have higher nuclear POP-1 levels than distal daughters. GFP::POP-1(Δ1-5) was used for *gon-14*, *gon-15*, and *gon-16*, each raised at 25°. GFP::POP-1(FL) was used for *sys-1* and *sys-3*, each raised at 20°. *gon-14(q686)* is shown; similar results were seen in *gon-14(q12)* raised at 25°.

2000). However, no function has been attributed to the other two Wnts, *cwn-1* and *cwn-2*. Perhaps one or both of these control the PD asymmetric cell division of Z1 and Z4. However, RNAi to either of these two genes gave no gonadogenesis defects (Siegfried and Kimble 2002). A second possibility is that a Wnt ligand common to AP cell divisions also controls Z1/Z4 polarity. In this scenario the initial signal by the Wnt may be refined by other factors or communication between Z1 and Z4 such that PD polarity rather than AP polarity is established. Third, a Wnt homolog may not be involved in controlling Z1/Z4 polarity. In this model, a cue inherent to the gonad is established on the basis of the AP and dorsal-ventral (DV) axes of the gonadal primordium (Siegfried and Kimble 2002).

Is a Wnt ligand involved in Z1/Z4 polarity? No Wnt ligand has been found to affect the polarity of the Z1/Z4 divisions (Siegfried and Kimble 2002; this work). Specifically, Z1/Z4 asymmetry was not affected by depletion of any of five known Wnt ligands or by depletion of two to three of these ligands in combination (Siegfried and Kimble 2002). Additionally, the single *porcupine* (*porc*) homolog, *mom-1*, which is required for Wnt function in the *C. elegans* embryo and in Drosophila (van den Heuvel *et al.* 1993; Rocheleau *et al.* 1997), has very minor defects in gonadogenesis (Siegfried and Kimble 2002). Because the gonadogenesis defects were rare in *mom-1* mutants, it was not determined whether these defects were due to a symmetrical division of Z1 and Z4.

In this work, we utilized genetic analysis to search for a role of Wnt in the control of Z1/Z4 polarity. We asked if *sys-1* or *pop-1* might interact genetically with either of two Wnt ligands or with *mom-1/porc*. We reasoned that analysis of a *mom-1/porc* mutant should represent the effect of removing all five Wnt genes. Therefore, the low-penetrance *mom-1* gonadogenesis defect might be dominantly enhanced by *sys-1* or *pop-1* if any of the Wnt ligands function in the asymmetric divisions of Z1 and Z4. However, no interactions were found. Although we cannot conclude that a Wnt ligand does not control Z1/Z4 polarity, at this time it seems unlikely.

Although a Wnt ligand may not function in the Z1/Z4 asymmetric division, there is precedence for a Wnt gene functioning more generally in gonadogenesis. A mutation affecting *lin-44*/Wnt was reported to enhance the gonadal defects in *tcl-2* mutants, suggesting that *lin-44* may have a role in gonadogenesis (Zhao *et al.* 2003). However, the *tcl-2* gene on its own does not have a Sys phenotype: DTCs were missing but extra ACs were not made (Zhao *et al.* 2003). Therefore, the *lin-44*/Wnt gene functions cooperatively with *tcl-2* in gonadogenesis; however, it may not control asymmetric division of Z1 and Z4.

Frizzled signaling decreases nuclear POP-1: POP-1 promotes distal fates among the Z1/Z4 daughters (Siegfried and Kimble 2002). One might therefore expect POP-1 to be more abundant in the nuclei of the distal daughter cells. However, the opposite is observed. After the asymmetric Z1/Z4 division, POP-1 is less abundant in distal nuclei than in proximal nuclei (this work). A similar phenomenon was observed in daughters of the T cells: POP-1 promotes the posterior fate of T.p, but nuclear POP-1 is lower in T.p than in its sister T.a (Meneghini *et al.* 1999; Rocheleau *et al.* 1999; Shin *et al.* 1999; Herman 2001). In both of these cases, loss of *pop-1* function has the same developmental defect as

the loss of Wnt/MAPK activities (Sawa *et al.* 1996; Rocheleau *et al.* 1999; Herman 2001; Siegfried and Kimble 2002). Therefore, Wnt/MAPK signaling positively regulates POP-1 function but reduces nuclear levels of POP-1 protein.

Regulation of TCF nuclear localization by Wnt signaling may be a conserved mechanism for modulating the function of TCF transcription factors. Nuclear POP-1 in *C. elegans* and nuclear Pangolin, the Drosophila TCF homolog, are both decreased in response to Wnt signaling (Lin *et al.* 1995, 1998; Rocheleau *et al.* 1997, 1999; Thorpe *et al.* 1997; Shin *et al.* 1999; Herman 2001; Chan and Struhl 2002; Maduro *et al.* 2002; Park and Priess 2003; and this work). This phenomenon was first discovered in the *C. elegans* embryo, which is complicated by POP-1 acting as an essential repressor in this case (Calvo *et al.* 2001; Maduro *et al.* 2002). Thus, in the embryonic EMS daughter cells, Wnt/MAPK signaling negatively regulates POP-1 repression of target genes. This negative regulation of POP-1 in the posterior daughter allows development of posterior fate. Therefore, the upstream Wnt signaling components have effects on cell fate opposite those of POP-1: removal of the Wnt ligand, Frizzled receptor, or β-catenin each results in both EMS daughters adopting the anterior fate, whereas removal of POP-1 results in both EMS daughters adopting the posterior fate (Lin *et al.* 1995; Rocheleau *et al.* 1997; Thorpe *et al.* 1997). Wnt signaling in the early embryo contrasts with that observed in postembryonic development. In postembryonic development, disruption of upstream Wnt signaling or POP-1 each has the same effect, suggesting that Wnt signaling positively regulates POP-1 function (Sawa *et al.* 1996; Rocheleau *et al.* 1997; Herman 2001; Siegfried and Kimble 2002). Similarly, in Drosophila, nuclear Pangolin/TCF is reduced by Wnt signaling and this reduction corresponds with positive regulation of Pangolin by Wnt signaling (Chan and Struhl 2002). The common theme is that Wnt signaling appears to decrease TCF in the nucleus of the activated cell. Depending on the context, reduction of nuclear TCF by Wnt signaling can either positively or negatively affect its function.

Models for regulation of POP-1 activation: Why is the level of nuclear POP-1 lower in cells whose fates are specified by POP-1? Current models assume that the TCF transcription factors act autonomously in the cell requiring its activity. If POP-1 does indeed act autonomously, then, in the *C. elegans* Z1/Z4 and T cell daughters and in the Drosophila embryo, low nuclear POP-1 represents the active form. Herman (2001) suggests that LIT-1 phosphorylates POP-1 in response to Wnt signaling and that this modification leads to both degradation and activation of POP-1. However, more recently, work in the *C. elegans* embryo suggests that reduction of nuclear POP-1 is not due to degradation (Maduro *et al.* 2002). Chan and Struhl (2002) have suggested that, in Drosophila, Armadillo/β-catenin activates Pangolin/TCF either by selectively exporting a repressor form of Pangolin from the nucleus or by activating Pangolin in the cytoplasm.

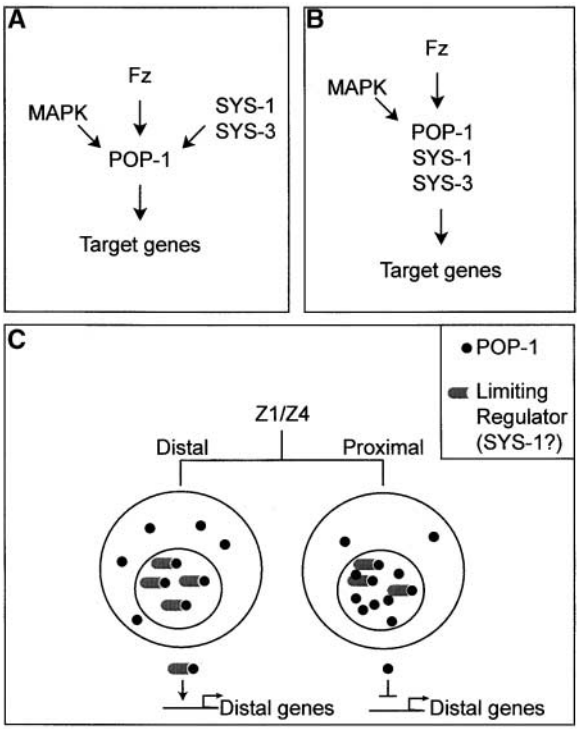

Figure 6.—Genetic and molecular models. (A and B) Two models of *sys-1* and *sys-3* in *frizzled* signaling. SYS-1 and SYS-3 do not control POP-1 asymmetry and therefore either function in parallel to WNT and MAPK signaling (A) or regulate POP-1 in the nucleus downstream of Wnt/MAPK regulation of POP-1 asymmetry (B). (C) SYS-1 may be a limiting coactivator of POP-1. POP-1 protein (solid circle) is less abundant in the nuclei of distal Z1/Z4 daughters compared to the proximal Z1/Z4 daughters. SYS-1 protein may be equally abundant in nuclei of all daughters, but present in limiting quantity. In the distal daughters the ratio of POP-1 to SYS-1 is about equal, and together these proteins activate distal genes. In the proximal daughters, POP-1 is more abundant than SYS-1 in the nucleus and less activator complex is made. On its own, POP-1 may repress distal genes and therefore outcompetes any SYS-1/POP-1 activator complex made.

We suggest a modified model to explain how a decreased level of nuclear POP-1 might favor an active form of the transcription factor (Figure 6C). This model incorporates our results with SYS-1, a dose-sensitive regulator of the pathway in Z1 and Z4. Both Herman (2001) and Chan and Struhl (2002) suggest that POP-1/Pangolin can exist in either an inactive or active form. Our model suggests that the ratio of active to inactive POP-1 is controlled by a coactivator that is present at a limiting concentration. By this model, POP-1 is not active when it is present at a high level, because most POP-1 is not bound to the limiting coactivator; instead, this form of POP-1 either is inactive or functions as a repressor. In contrast, POP-1 is active when present at a low level, because most POP-1 can bind to the limiting coactivator.

An attractive idea is that SYS-1 might be the limiting transcriptional coactivator. Evidence supporting this idea is: (1) *sys-1* specifies the same fate as Wnt/MAPK regulators; (2) *sys-1* displays a dramatic genetic interaction with *pop-1*, which may indicate a physical interaction between SYS-1 and POP-1 proteins; (3) *sys-1* is a dose-sensitive locus; and (4) *sys-1* does not affect POP-1 asymmetry. Therefore, although the molecular role of SYS-1 is not known, its genetic properties are consistent with a role as a POP-1 coactivator present at limiting concentration. One test of this model might have been to increase *sys-1* dosage using a duplication; however, duplications of this region are unstable. Instead, we recently cloned *sys-1* (T. Kidd, unpublished data) and plan to test the model by overexpression of a *sys-1* transgene.

***sys-1* and *sys-3* function in parallel with or downstream of POP-1 to regulate Z1/Z4 asymmetric divisions:** In this work we report identification of a new gene, *sys-3*, that controls Z1/Z4 polarity. We provide evidence suggesting that *sys-1* and *sys-3* act together with Wnt/MAPK signaling in the Z1/Z4 daughters. Specifically, we have shown that *sys-1* has dominant genetic interactions with *pop-1* and *lin-17* while *sys-3* has dominant genetic interactions with *sys-1* and *pop-1*. The similar mutant phenotypes shared by *sys-1*, *sys-3*, *pop-1*, and *lin-17* together with the dominant genetic interactions suggest that *sys-1* and *sys-3* function in the Wnt signaling cascade with *pop-1* and *lin-17*. Alternatively, one or both of the *sys-1* and *sys-3* genes function in a parallel pathway that is required for Wnt signaling. For example, these pathways may converge to cooperatively activate target genes.

The function of *sys-1* and *sys-3* appears to be distinct from that of upstream Wnt/MAPK regulators of POP-1. Thus, *lin-17*, *wrm-1*, and *lit-1* all promote POP-1 asymmetry (Figure 2), but *sys-1* and *sys-3* do not affect POP-1 asymmetry (Figure 5). Although the *sys-1* and *sys-3* alleles used in these assays may not be nulls, they nonetheless render the Z1/Z4 division symmetric without affecting POP-1 asymmetry (Miskowski *et al.* 2001; this work). Therefore, *sys-1* and *sys-3* are likely to act in parallel to the Wnt/MAPK regulators of POP-1 (Figure 6A), together with POP-1 (Figure 6B), or downstream of POP-1 (not shown).

***gon-14*, *gon-15*, and *gon-16*: a role in Z1/Z4 polarity?** We have isolated mutations in three genes, *gon-14*, *gon-15*, and *gon-16*, which are missing DTCs and display a Sys-like SPh defect. Furthermore, *sys-1* and *pop-1* mutations can dominantly enhance gonadal defects in *gon-14*, *gon-15*, and *gon-16* homozygotes. Therefore, these genes may influence POP-1 and SYS-1 function. However, *gon-14*, *gon-15*, and *gon-16* mutants do not produce extra cells with a proximal fate and therefore may not cause the distal-to-proximal fate transformations seen in *sys* mutants. Alternatively, *gon-14*, *gon-15*, and *gon-16* genes may control Z1/Z4 polarity as well as later steps critical for gonadogenesis, such as DTC and AC differentiation or maintenance. Such a later function is suggested by weak *lag-2:GFP* expression in some DTCs and weak *cdh-3::GFP* expression in some ACs.

We thank Laura Mathies, Finn-Hugo Markussen, Peggy Kroll-Conner, and Lisa Friedman for participation in the gonadogenesis screen that generated mutations in *sys-3*, *gon-14*, *gon-15*, and *gon-16*. We thank Joel Rothman and Morris Maduro for providing plasmids and discussing unpublished data, Jennifer Miskowski for providing *jmp#1*, and Andy Fire for plasmids. We also thank Laura Mathies and Daniel Hesselson for critical comments on the manuscript and Alison Blackwelder and Joseph Anderson for technical assistance. Some strains used in this work were supplied by the *C. elegans* stock center (Caenorhabditis Genetics Center). K.R.S., A.R.K., and M.A.C. were trainees of National Institutes of Health training grants, Genetics (GM07133), Molecular Biosciences (GM07215), and Biotechnology (GM08349), respectively. J.K. is an investigator with the Howard Hughes Medical Institute.

LITERATURE CITED

Blelloch, R., S. Santa Anna-Arriola, D. Gao, Y. Li, J. Hodgkin *et al.*, 1999 The *gon-1* gene is required for gonadal morphogenesis in *Caenorhabditis elegans*. Dev. Biol. **216:** 382–393.

Brenner, S., 1974 The genetics of *Caenorhabditis elegans*. Genetics **77:** 71–94.

Calvo, D., M. Victor, F. Gay, G. Sui, M. P.-S. Luke *et al.*, 2001 A POP-1 repressor complex restricts inappropriate cell type-specific gene transcription during *Caenorhabditis elegans* embryogenesis. EMBO J. **20:** 7197–7208.

Chan, S.-K., and G. Struhl, 2002 Evidence that Armadillo transduces Wingless by mediating nuclear export or cytosolic activation of Pangolin. Cell **111:** 265–280.

Friedman, L., S. Santa Anna-Arriola, J. Hodgkin and J. Kimble, 2000 *gon-4*, a cell lineage regulator required for gonadogenesis in *Caenorhabditis elegans*. Dev. Biol. **228:** 350–362.

Greenwald, I., 1998 LIN-12/Notch signaling: lessons from worms and flies. Genes Dev. **12:** 1751–1762.

Herman, M. A., 2001 *C. elegans* POP-1/TCF functions in a canonical Wnt pathway that controls cell migration and in a noncanonical Wnt pathway that controls cell polarity. Development **128:** 581–590.

Herman, M. A., and H. R. Horvitz, 1994 The *Caenorhabditis elegans* gene *lin-44* controls the polarity of asymmetric cell divisions. Development **120:** 1035–1047.

Hodgkin, J., 1997 Appendix 1. Genetics, pp. 881–1047 in *C. elegans II*, edited by D. L. Riddle, T. Blumenthal, B. J. Meyer and J. R. Priess. Cold Spring Harbor Laboratory Press, Cold Spring Harbor, NY.

Hubbard, E. J. A., and D. Greenstein, 2000 The *Caenorhabditis elegans* gonad: a test tube for cell and developmental biology. Dev. Dyn. **218:** 2–22.

Kaletta, T., H. Schnabel and R. Schnabel, 1997 Binary specification of the embryonic lineage in *Caenorhabditis elegans*. Nature **390:** 294–298.

Kimble, J., 1981 Alterations in cell lineage following laser ablation of cells in the somatic gonad of *Caenorhabditis elegans*. Dev. Biol. **87:** 286–300.

Kimble, J., and D. Hirsh, 1979 The postembryonic cell lineages of the hermaphrodite and male gonads in *Caenorhabditis elegans*. Dev. Biol. **70:** 396–417.

Kimble, J. E., and J. G. White, 1981 On the control of germ cell development in *Caenorhabditis elegans*. Dev. Biol. **81:** 208–219.

Lin, R., S. Thompson and J. R. Priess, 1995 *pop-1* encodes an HMG box protein required for the specification of a mesoderm precursor in early C. elegans embryos. Cell **83:** 599–609.

Lin, R., R. J. Hill and J. R. Priess, 1998 POP-1 and anterior-posterior fate decision in *C. elegans* embryos. Cell **92:** 229–239.

Maduro, M., and D. Pilgrim, 1995 Identification and cloning of *unc-119*, a gene expressed in the *Caenorhabditis elegans* nervous system. Genetics **141:** 977–988.

Maduro, M. F., R. Lin and J. H. Rothman, 2002 Dynamics of a developmental switch: recursive intracellular and intranuclear

redistribution of *Caenorhabditis elegans* POP-1 parallels Wnt-inhibited transcriptional repression. Dev. Biol. **248:** 128–142.

Meneghini, M. D., T. Ishitani, J. C. Carter, N. Hisamoto, J. Ninomiya-Tsuji *et al.*, 1999 MAP kinase and Wnt pathways converge to downregulate an HMG-domain repressor in *Caenorhabditis elegans*. Nature **399:** 793–797.

Miskowski, J., Y. Li and J. Kimble, 2001 The *sys-1* gene and sexual dimorphism during gonadogenesis in *Caenorhabditis elegans*. Dev. Biol. **230:** 61–73.

Niswander, L., 2002 Interplay between the molecular signals that control vertebrate limb development. Int. J. Dev. Biol. **46:** 877–881.

Park, F. D., and J. R. Priess, 2003 Establishment of POP-1 asymmetry in early *C. elegans* embryos. Development **130:** 3547–3556.

Pettitt, J., W. B. Wood and R. H. A. Plasterk, 1996 *cdh-3*, a gene encoding a member of the cadherin superfamily, functions in epithelial cell morphogenesis in *Caenorhabditis elegans*. Development **122:** 4149–4157.

Praitis, V., E. Casey, D. Collar and J. Austin, 2001 Creation of low-copy integrated transgenic lines in *Caenorhabditis elegans*. Genetics **157:** 1217–1226.

Rocheleau, C. E., W. D. Downs, R. Lin, C. Wittmann, Y. Bei *et al.*, 1997 Wnt signaling and an APC-related gene specify endoderm in early C. elegans embryos. Cell **90:** 707–716.

Rocheleau, C. E., J. Yasuda, T. H. Shin, R. Lin, H. Sawa *et al.*, 1999 WRM-1 activates the LIT-1 protein kinase to transduce anterior/posterior polarity signals in *C. elegans*. Cell **97:** 717–726.

Sawa, H., L. Lobel and H. R. Horvitz, 1996 The *Caenorhabditis elegans* gene *lin-17*, which is required for certain asymmetric cell divisions, encodes a putative seven-transmembrane protein similar to the *Drosophila* Frizzled protein. Genes Dev. **10:** 2189–2197.

Shin, T. H., J. Yasuda, C. E. Rocheleau, R. Lin, M. Soto *et al.*, 1999 MOM-4, a MAP kinase kinase kinase-related protein, activates WRM-1/LIT- 1 kinase to transduce anterior/posterior polarity signals in *C. elegans*. Mol. Cell **4:** 275–280.

Siegfried, K., and J. Kimble, 2002 POP-1 controls axis formation during early gonadogenesis in *C. elegans*. Development **129:** 443–453.

Sternberg, P. W., and H. R. Horvitz, 1988 *lin-17* mutations of *Caenorhabditis elegans* disrupt certain asymmetric cell divisions. Dev. Biol. **130:** 67–73.

Sulston, J. E., and H. R. Horvitz, 1977 Post-embryonic cell lineages of the nematode, *Caenorhabditis elegans*. Dev. Biol. **56:** 110–156.

Tabara, H., M. Sarkissian, W. G. Kelly, J. Fleenor, A. Grishok *et al.*, 1999 The *rde-1* gene, RNA interference, and transposon silencing in *C. elegans*. Cell **99:** 123–132.

Thorpe, C. J., A. Schlesinger, J. C. Carter and B. Bowerman, 1997 Wnt signaling polarizes an early C. elegans blastomere to distinguish endoderm from mesoderm. Cell **90:** 695–705.

van den Heuvel, M., C. Harryman-Samos, J. Klingensmith, N. Perrimon and R. Nusse, 1993 Mutations in the segment polarity genes *wingless* and *porcupine* impair secretion of the wingless protein. EMBO J. **12:** 5293–5302.

Whangbo, J., J. Harris and C. Kenyon, 2000 Multiple levels of regulation specify the polarity of an asymmetric cell division in *C. elegans*. Development **127:** 4587–4598.

Zhao, X., H. Sawa and M. A. Herman, 2003 *tcl-2* encodes a novel protein that acts synergistically with Wnt signaling pathways in *C. elegans*. Dev. Biol. **256:** 276–289.

Communicating editor: B. J. Meyer